A statistical comparison of coupled thermosphere-ionosphere models

Lucas Liuzzo

April 29, 2014

1 Introduction

The thermosphere-ionosphere system is a highly dynamic, non-linearly coupled interaction that fluctuates on a daily basis. Many models exist to attempt to quantify the relationship between the two atmospheric layers, and each approaches the problem differently. Such models range from empirical models like IRI [*Rawer, Bilitza, and Ramakrishnan*, 1978; *Bilitza*, 2001] to data assimilation models like GAIM [*Schunk et al.*, 2004] and physics-based, coupled thermosphere-ionosphere models like TIE-GCM [*Richmond, Ridley, and Roble*, 1992], CTIPe [*Millward et al.*, 2001], and GITM [*Ridley, Deng, and Tòth*, 2006]. Because each of these models differs in the implementation of the equations that govern the dynamics of the thermosphere-ionosphere system, it is important to understand under which conditions each model performs best, and under which conditions each model may have limitations in accuracy. With this in consideration, this study examines the ability of two of the leading coupled thermosphere-ionosphere models in the community to reproduce observed thermospheric and ionospheric quantities during times of differing geomagnetic activity. The methods and models are briefly examined initially, followed by a description of the techniques used to compare the models. Next, model results from each of the three geomagnetically active periods are presented, followed by quantitative errors and prediction efficiencies of each model at high, mid, and low latitudes.

2 Methods

Two coupled thermosphere-ionosphere models, the Thermosphere/Ionosphere General Circulation Model with coupled electrodynamics (TIE-GCM) and the Global Ionosphere-Thermosphere Model (GITM), will be directly compared to test the accuracy of each model during three geomagnetic conditions. Because models can behave differently during times with different geomagnetic activity, model results during multiple days ranging from low to high activity are explored. The first period compared is a highly-active time, with a maximum Planetary K-index value (Kp) of 7; second is a time period with moderate activity, with a Kp of 4. Finally, a quiet time period will be compared, during which a Kp of 0 was measured. The storms and their descriptions are available in Table 1. The dates that are compared in this study correspond to an electrodynamics thermosphere ionosphere (EIT) challenge initiated by the coupling energetics and dynamics of atmospheric regions (CEDAR) program, and a recent publication by *Shim et al.* [2014] presents the complete findings of the challenge. The main difference in this study is the version of GITM that is used to model the thermosphere and ionosphere is more recent. However, to allow for direct comparison between the

Table 1: Definition of storms studied along with geomagnetic activity levels.

Activity Level	Name	Date and Time	$F_{10.7}$	Max Kp
Strong	20050831	31 Aug 2005 10:00 UT to 01 Sepr 2005 12:00 UT	86	7
Moderate	20010831	31 Aug 2001 00:00 UT to 01 Sep 2001 00:00 UT	192	4
Quiet	20070709	09 Jul 2007 00:00 UT to 10 Jul 2007 00:00 UT	80	0

findings presented here and the results of the CEDAR EIT challenge, these results will be presented using similar metrics to quantify the differences.

2.1 Validation

To compare the ability of each model to replicate the near-Earth space environment, data from the CHallenging Minisatellite Payload satellite (CHAMP) is used exclusively as truth for each activity level compared. CHAMP is a German satellite that was launched in July of 2000, and its payload includes a magnetometer, accelerometer, Global Positioning System (GPS) receiver, and ion drift meter. Using GPS radio occultation techniques, the satellite is able to measure spatial densities in neutral and electron constituents. Because of the accessibility of these datasets, two quantities are directly compared between the models: neutral density and electron density, each measured at the satellite's altitude and orbital location. The data used is collected in 3° bins, corresponding to the motion of the satellite over the planet as it orbits. The orbit of the satellite is at an approximately 87° inclination angle, with a period of 94 minutes and an altitude of about 450 km at launch. The orbital period causes daily fluctuations in the data to be overpowered by the variations in the data due to the satellite's orbit, because the quantities (such as density, for example) are highly dependent on the satellite's location in local time (see Figure 1). Therefore, to alleviate this, a low-pass, running-average filter with a 94 minute window is applied to the data to remove any orbital dependencies of the satellite. This allows for a more clear interpretation of the changes due to storm effects as opposed to changes due to local time of the satellite. This type of orbital filtering will be used throughout the study when visually comparing the two models with CHAMP observed data, but it is not used in comparing the two models quantitatively; that is, the parameters presented in Sections 2.3 and 3.5 do not use the smoothed data to obtain their values.

2.2 Models

There are many models that solve for the dynamics of the thermosphere-ionosphere system using equations that can be vastly different from one another. The Community Coordinated Modeling Center (CCMC) houses nine of these models alone, and many others exist that are not available through the CCMC. In addition, many of the models at CCMC have newer, updated versions that are run at their respective institutions, and thus differ from the models at the CCMC. Because of these variations, it is highly important to be able to provide validation of multiple models during differing geomagnetic conditions to understand the accuracy and limitations of the models. Thus study will present a direct comparison of two of the more widely-used models: TIE-GCM and GITM. While both models are similar in that they couple the dynamics of the thermosphere and ionosphere system, each model does so using different techniques. In some cases, the differences in how the models solve the set of equations that describes the coupling of the two atmospheric layers leads to drastically disparate results.

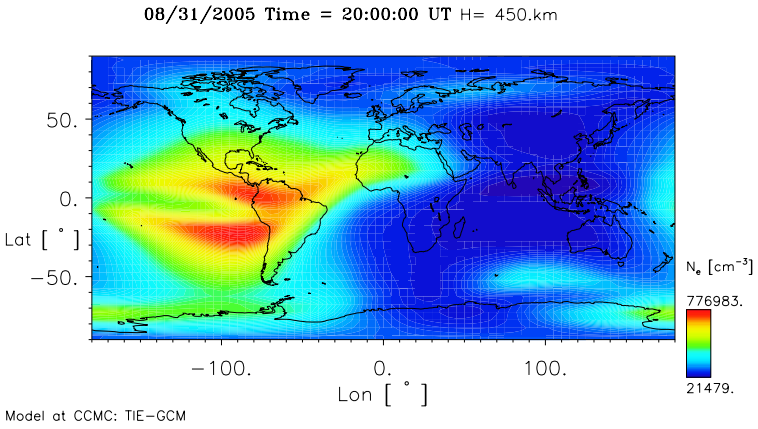

(a) Global electron density modeled by TIE-GCM.

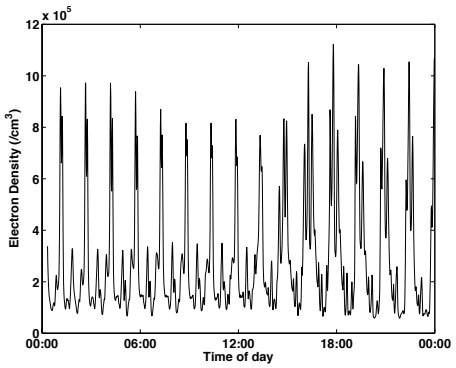

(b) Electron density measured by CHAMP.

Figure 1: Typical values of electron density at the CHAMP satellite altitude during a day (1a). Variations in density measured by CHAMP as the satellite moves in a polar orbit around the Earth (1b).

To model the thermosphere-ionosphere interaction, TIE-GCM makes use of the hydrostatic approximation, namely

$$\frac{dp}{dz} = -\rho g. \tag{1}$$

In doing so, the model solves for the global distribution of both neutral and ionized atomic and molecular constituents in the form of number densities, the neutral, ion, and electron temperatures, and constant pressure surface altitudes. By assuming a hydrostatic atmosphere and solving for these constant pressure surfaces, the model implements a pressure grid coordinate system. The scale of the model ranges from 97 to 500 km in altitude, using 29 surfaces of constant pressure in intervals of half scale heights. In the latitude-longitude direction, a $5^\circ \times 5^\circ$ grid resolution is used. To solve for the electrodynamics of the system, two approaches are implemented. At high latitudes above a constant critical colatitude, TIE-GCM uses an imposed electric field model as defined by *Heelis, Lowell, and Spiro* [1982]. Equatorward of the high-latitude region, a self-consistent dynamo solution is used for the electric fields. The auroral precipitation of the model is obtained from variation in the 3-hour Kp index, in the form of hemispheric power in GW.

Unlike TIE-GCM, GITM does not assume a hydrostatic atmosphere described by Equation 1. In doing so, constant pressure surfaces are not solved; rather, an altitude-based grid is implemented. The grid used for these runs range from approximately 96 to 700[1]km, with about 60 spacings between the two extremes. The resolution in the longitudinal and latitudinal direction is slightly finer than the TIE-GCM model, set at $5^\circ\times \sim 3^\circ$, respectively. The electrodynamic solver used within GITM is similar to that used within TIE-GCM, in that an electric potential pattern is imposed at high-latitudes, but is described by *Weimer* [2005]. Equatorward of a critical magnetic colatitude defined to be 65°, a self-consistent dynamo solution is used to solve for the electric fields within the model. Auroral precipitation in the GITM runs is defined by the *Fuller-Rowell and Evans* [1987] model.

The results from the TIE-GCM model runs are publicly available and obtained through the CCMC

[1]Because of the stretched altitudinal grid that GITM uses, this upper boundary is variable, and highly dependent on the amount of solar activity and initial drivers used in the model.

webpage (http://ccmc.gsfc.nasa.gov), where the results from each run during the events studied are hosted. In addition to the availability of 20-minute output files of the model variables along the orbital path of CHAMP, interpolated data up to a 1 second resolution is available. For this study, interpolated data with a resolution of 1 minute is used. This interpolation flies a satellite along the CHAMP orbit through the entire 3D output files of the model to obtain the data at a finer resolution along the satellite trajectory. The results from the GITM model runs are run using NASA's High-End Computing Capability (http://nas.nasa.gov/hecc). Because the GITM runs are initialized locally, there is more control of the data output along the satellite path. As opposed to a 20-minute interpolation of the data, quantities along the CHAMP orbit are output at every minute to avoid this interpolation.

In addition to the interpolation described above, a further correction must be made for both models. Because the champ data used for this study is obtained as an average of the readings from a 3° bin and not necessarily at one minute intervals, the model must be fixed to be directly compared to the CHAMP data. This interpolation is quickly performed locally. The densities of neutrals and electrons along the CHAMP trajectory are thus a direct output of each model once the interpolations have been performed. With the data from each model in these forms, the ability of the two models to reproduce observed data sets can be directly compared.

2.3 Comparison Techniques

A few various quantities will be used to compare the differences between the TIE-GCM and GITM runs for each day. The first is a root-mean-square difference, defined as

$$\mathrm{RMS} = \sqrt{\frac{\sum (x_{\mathrm{obs}} - x_{\mathrm{mod}})^2}{N}}, \tag{2}$$

where N is the number of data points used in the subtraction, and the subscripts 'obs' and 'mod' refer to the observed and modeled data, respectively. Therefore, an RMS difference has a range from $0 < \mathrm{RMS} < \infty$ in units of the quantity compared, with 0 being a perfect value for the difference. The second parameter used is a dimensionless parameter called prediction efficiency, defined to be

$$\mathrm{PE} = 1 - \frac{\mathrm{RMS}_{\mathrm{mod}}}{\mathrm{RMS}_{\mathrm{mean}}} = 1 - \sqrt{\frac{\sum (x_{\mathrm{obs}} - x_{\mathrm{mod}})^2/N}{\sum (x_{\mathrm{obs}} - < x_{\mathrm{obs}} >)^2/N}}, \tag{3}$$

where $< x_{\mathrm{obs}} >$ is the mean of the observed CHAMP data. Clearly, the prediction efficiency is a metric used to determine whether the model or the average of the data is better at representing the trends in the data. The prediction efficiency ranges from $-\infty < \mathrm{PE} \leq 1$, with 1 being a perfect predictor. Values less than zero suggest that the mean of the data is more accurate at representing trends than the model is. Because of the orbital trajectory of the satellite, both the RMS difference and PE will be presented in three regions: the high-latitude region, mid-latitude region, and equatorial region. This allows for the comparison of model accuracy at multiple locations at a range of geomagnetic activity levels. High-latitude regions are defined to be above 50°, mid-latitude is the region between 25° and 50°, and the equatorial region are latitudes below 25°. Both hemispheres are included in the error calculations. The findings for RMS and PE will be presented in Section 3.5.

A final value is used to qualitatively observe trends between the model and data, and is in the form of a difference between CHAMP and modeled quantities. This difference allows for a quick

interpretation of how well each model represents the quantity being compared, and how well the model reacts to changes in geomagnetic condition. Unlike an RMS difference, this straight difference can become negative, and thus range between $-\infty$ and ∞, with a perfect value of 0. The findings for the difference errors will be presented in Sections 3.2–3.4.

3 Results and Discussion

3.1 Expected Results

The interaction between the thermosphere and ionosphere is highly complicated, yet certain trends are expected during various levels of geomagnetic activity, and will be briefly explained here. During a storm event, the amount of ionized particles that precipitate into the magnetosphere and ionosphere significantly increases due to an increased rate of magnetic reconnection on both the day- and night-side of the Earth. These particles gyrate along field lines as the field lines precess around the Earth, following what is known as a Dungey Cycle [*Dungey*, 1961]. A particle can then enter the loss cone of the field line, causing it to be deposited into the ionosphere. Once lost, one of three things can happen: ionization, excitation, or recombination. Ionization occurs when the charged particle collides with an atmospheric neutral and strips off an electron from the neutral. This process creates an additional charged particle in the ionosphere. Excitation occurs when the precipitating particle collides with a neutral but lacks the energy required to completely strip the neutral of an electron. However, the particle contains enough energy to excite the electrons of the neutral to higher, less stable energy states. After a time, this unstable energy state decays and the electrons go to a lower energy, and in doing so emit a pulse of light. This is known as the aurora. These two processes indicate why auroral activity drastically increases during geomagnetic events. In addition to the increased aurora, it is clear that an increase in charged particles throughout the ionosphere will occur. Thus, during geomagnetic events, we might expect the number density of electrons in the ionosphere to increase. The third process, recombination, is a necessary step in turning positively charged ions into neutrals. As an electron precipitates from the loss cone of the magnetosphere into the ionosphere, it may collide with a positively charged ion. This collision causes the electron and ion to recombine, and to form a neutral constituent of the atmosphere. Thus, with increased geomagnetic activity and particle population, we would expect the neutral densities of the thermosphere to increase. Generally, this is the type of behavior that will be shown to exist in the CHAMP data in Sections 3.2–3.4, but may or may not occur in the model results during these times.

3.2 Strong Event

The event occurring on 31 August, 2005 is classified as a strong event. On this day, a high speed stream (HSS) of solar wind impacted the Earth system, causing widespread geomagnetic activity. As described above, the expected behavior of the neutral and electron population within the thermosphere-ionosphere system is to increase.

Figure 2 shows the results of CHAMP data compared with both the GITM and TIE-GCM model for the neutral (2a) and electron (2b) particle populations. As expected, when looking at neutrals observed by the CHAMP satellite, a significant increase in neutral density is observed beginning around 10:00 UT. Throughout the day, GITM models the observed data well, and shows an increase

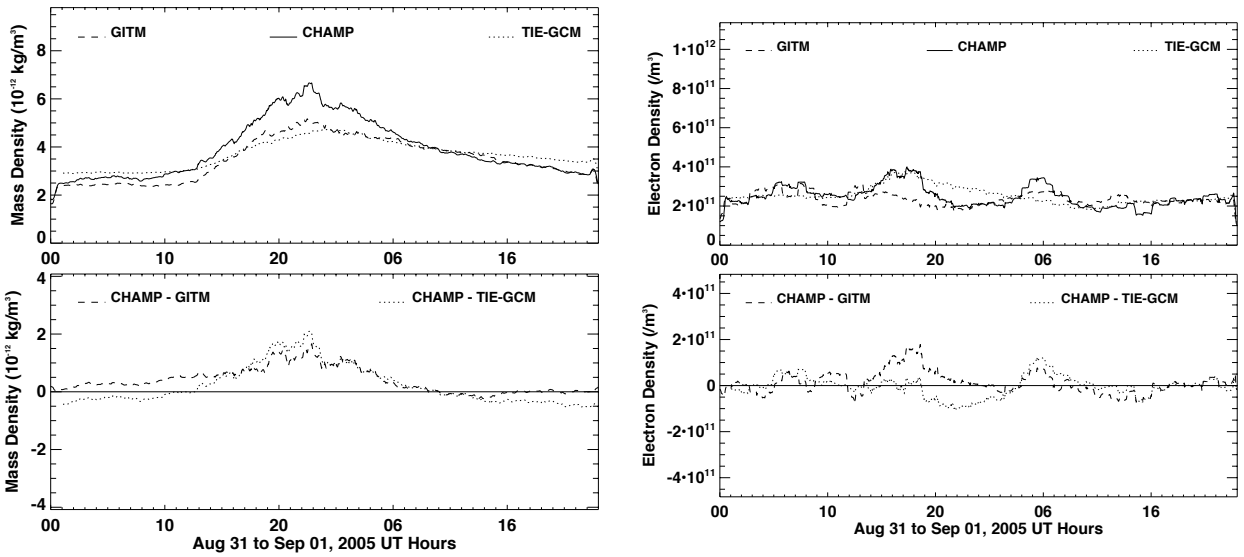

(a) (b)

Figure 2: Neutral (2a) and electron (2b) densities along the CHAMP satellite path for the strong event. The difference between CHAMP and each model is plotted below the direct comparison. Both models capture the increase in neutral density during the storm, but underestimate the storm-time neutral density. In modeling the electron density, TIE-GCM is closer to the observed density at the start of the storm, while GITM is closer to the observed density toward the end of the event.

in density slightly after the observed density increase at 13:00 UT. TIE-GCM models an increase around 13:00 UT as well. However, it is clear that in both cases, the extent of the density increase is not completely captured in either model, as both models underestimate the amount of neutrals in the system. As the storm begins to subside, both models accurately replicate the observed neutral density, with TIE-GCM slightly overestimating the density after the event has ended. For the electron density, both models capture the electron densities well before the event starts. As time increases, the amount of error between CHAMP and GITM increases, especially during the beginning of the storm event, where GITM underestimates the observed densities. After the event begins to subside around 05:00 UT on Sep 01, the densities produced by GITM are close to the observed electron density. Unlike GITM, TIE-GCM replicates the electron densities best during the event, but toward the end of the event overestimates the amount of electrons in the system.

3.3 Moderate Event

The event occurring on 31 August, 2001 was driven by a shock-front of a passing Coronal Mass Ejection (CME) resulting from extremely strong flare activity (reaching a peak of X5) six days prior. Because the CME erupted from the southeastern limb it only glanced the Earth's magnetosphere, but was nonetheless geoeffective. Since this is a moderate event, there may be a slight increase in neutral and electron density observed by the CHAMP satellite.

As before, we focus first on the neutral and electron particle populations, followed by the cross-track winds. Figure 3a (3b) shows the neutral (electron) densities of the CHAMP satellite and models during the moderate event. For this event, GITM captures the slight increase in density that is observed by CHAMP that peaks around 10:00 UT. TIE-GCM, however, models a near

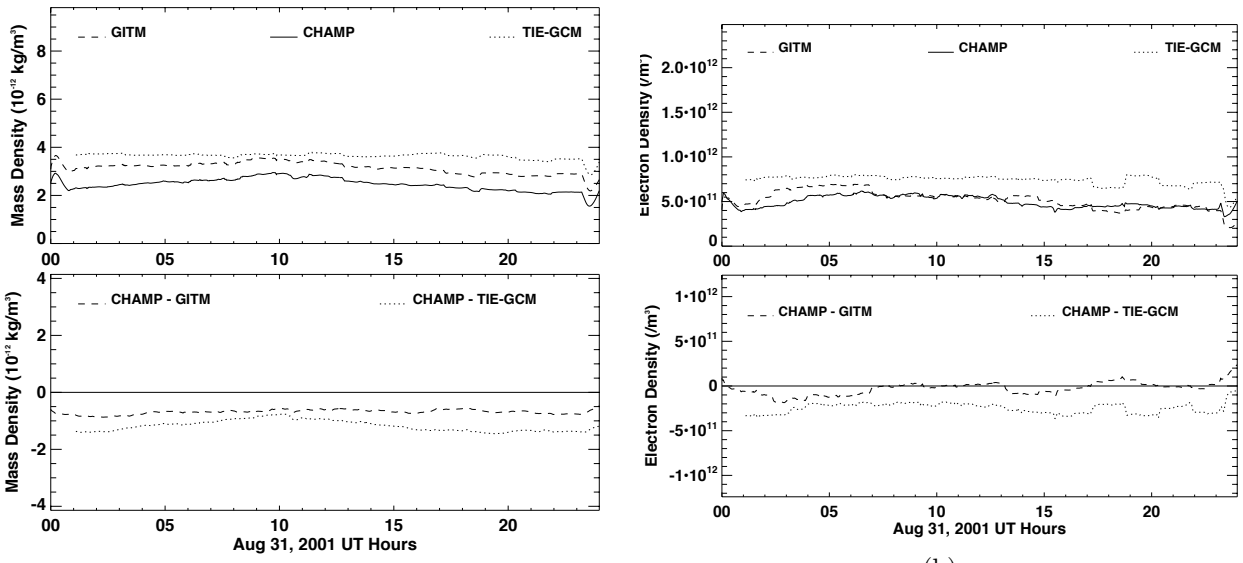

(a) (b)

Figure 3: Same as Figure 2 but for the moderate event. A slight increase in the neutral density is modeled by GITM but not TIE-GCM during the event, but both models overestimate the density observed by CHAMP. In modeling the electron population, GITM is much closer to the observed density throughout the event.

constant thermospheric density throughout the day. Whereas for the strong event both models underestimated the neutral density value, both GITM and TIE-GCM overestimate the amount of neutrals in the thermosphere. For the electron density comparisons, GITM is much closer to predicting the densities throughout the entire day, whereas in the strong event it was only accurate toward the end of the storm. As with neutral densities, TIE-GCM models a near constant electron density population along the CHAMP trajectory, and shows minimal changes until toward the end of the event.

3.4 Quiet Event

For the quiet event in July, Figure 4a shows the neutral density and Figure 4b shows the electron density observed by CHAMP and modeled by GITM and TIE-GCM. GITM shows very good agreement with the CHAMP observed densities throughout the event, whereas TIE-GCM significantly overestimates the amount of neutrals within the thermosphere. For the quiet event, TIE-GCM models the electron density closely: a significant increase in accuracy compared to the events with strong and moderate geomagnetic activity. GITM similarly agrees with the CHAMP electron density, but is in slightly less agreement than the previous two events. However, both models overestimate the electron density during most of the day.

3.5 Error Results

Presented in the previous section were event-long, qualitative differences between the data and two models. This section will present both root-mean-square differences and prediction efficiencies

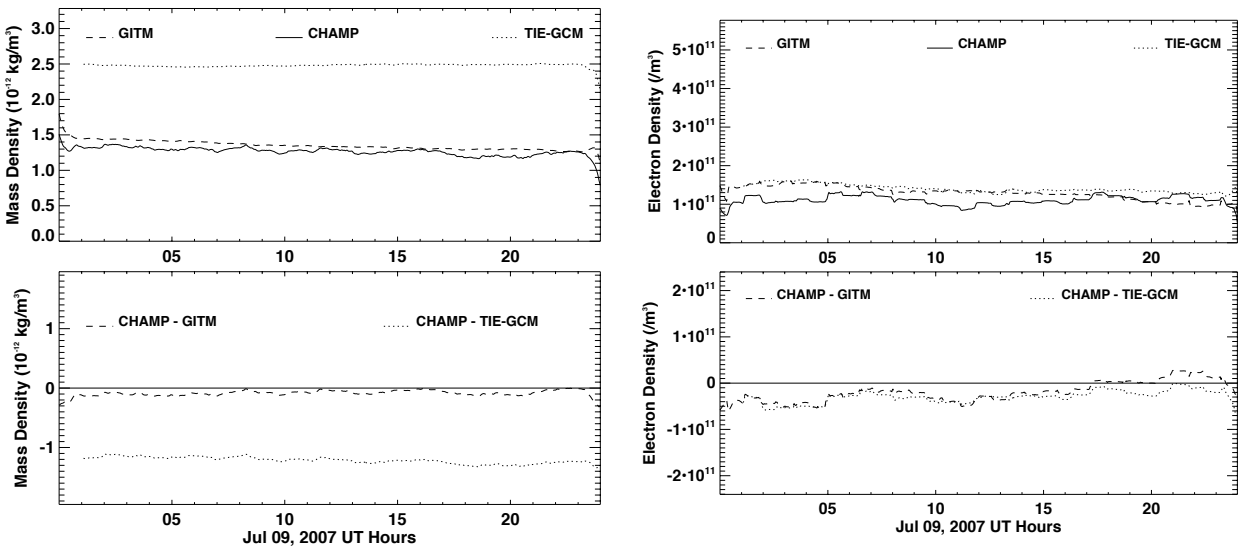

(a) (b)

Figure 4: Same as Figure 2 but for the quiet event. GITM closely models the observed neutral density throughout the event, but TIE-GCM is significantly higher than the observed density. Both models slightly overestimate the electron density during the event, but accuracy increases toward the end of the day.

for each model when compared with CHAMP, at high, mid, and low latitudes along the CHAMP trajectory. Tables 2 and 3 present the results of RMS and PE for neutral and electron density. For all geomagnetic conditions, GITM is better at modeling the neutral density of the thermosphere, as the RMS and PE values for GITM are often an order of magnitude better than those for TIE-GCM. In addition, GITM has the highest prediction efficiency at all latitudes during the strong period, and has the smallest RMS difference at all latitudes during the quiet period. However, TIE-GCM is often more accurate a lower latitudes than at middle or high latitudes. For the electron density during the strong, moderate, and quiet events, GITM is able to more accurately predict the behavior that is observed by CHAMP and has lower RMS differences. Again, TIE-GCM is frequently better at reproducing the electron density at lower latitudes than at other locations, and is much closer to CHAMP in modeling electrons than in modeling the neutral density. It is clear that the different models are better at predicting the behavior of the thermosphere-ionosphere system during different conditions, and because of the equations solved and the assumptions inherent to each model, different results for different periods will exist.

4 Conclusion

A direct comparison and validation study of the Thermosphere/Ionosphere General Circulation Model with coupled electrodynamics and the Global Ionosphere-Thermosphere Model has been presented here. The validation is preformed using observational data from the CHallenging Minisatellite Payload satellite, during three time periods that each differ in the geomagnetic activity level. In general, at times of high geomagnetic activity, both models underestimate the observed neutral density population, and are closer to but overestimate the density during all other geomagnetic conditions, with GITM closer to the observed CHAMP data. The prediction efficiencies of

Table 2: Neutral density RMS differences (10^{-12} kg/m^3) and PE of GITM and TIE-GCM for each event studied at high, mid, and low latitude regions of the CHAMP orbit.

		Strong		Moderate		Quiet	
Latitude	Model	RMS	PE	RMS	PE	RMS	PE
High	GITM	1.14	0.348	0.868	0.595	0.453	0.167
	TIE-GCM	1.75	−0.00175	3.78	−0.763	1.36	−1.51
Middle	GITM	0.917	0.475	0.953	0.556	0.465	0.145
	TIE-GCM	1.60	0.0835	3.64	−0.700	1.42	−1.61
Low	GITM	0.689	0.605	0.895	0.582	0.465	0.145
	TIE-GCM	1.380	0.209	3.41	−0.593	1.41	−1.60

Table 3: Electron density RMS differences (10^{11} /m^3) and PE of GITM and TIE-GCM for each event studied at high, mid, and low latitude regions of the CHAMP orbit.

		Strong		Moderate		Quiet	
Latitude	Model	RMS	PE	RMS	PE	RMS	PE
High	GITM	2.29	0.156	2.62	0.525	1.16	−0.135
	TIE-GCM	4.02	−0.479	10.4	−0.883	1.69	−0.663
Middle	GITM	1.89	0.303	4.36	0.211	1.24	−0.222
	TIE-GCM	3.72	−0.370	9.63	−0.745	1.78	−0.744
Low	GITM	2.06	0.242	4.49	0.187	1.26	−0.234
	TIE-GCM	3.19	−0.176	10.2	−0.854	1.70	−0.674

neutral density for both models during all levels of activity are significantly higher than for electron density. The underestimation observed during the strong storm could be the cause of the drivers initialized in each model, as drivers that work well in low and moderate geomagnetic activity may be too conservative in their particle precipitation, as the auroral precipitation models used for each model have limited ability to create strong precipitation. For electron density, the models are closer to reproducing the observed density values than with neutrals, however the profile of the density change throughout the day is often not correctly replicated, and is visible in the lower prediction efficiency values. In examining the event results presented here, GITM is better at predicting neutral and electron densities during the strong and moderate event, but TIE-GCM is better at predicting the densities during the quiet event. However, GITM is closer in reproducing the actual densities observed by CHAMP for all events, as reflected in the RMS values at all latitudes. Despite solving for the same parameters, the differences in the model assumptions (including hydrostatic equilibrium, the use of different grids, and disparate high-latitude potential solvers) causes the models to obtain drastically different results during each of the events. In addition, it is clear from the results found here and in the study by *Shim et al.* [2014] that the evolution of GITM continues to improve its accuracy.

Acknowledgements

The author would like to thank the staff at the Community Coordinated Modeling Center for providing the data used for the TIE-GCM runs, accessible through the run database located on the CCMC website (http://ccmc.gsfc.nasa.gov). He would also like to thank Professors Michael Liemohn and Aaron Ridley of the University of Michigan, and Dr. Ja Soon Shim of the Goddard Space Flight Center for helpful discussion and guidance throughout the study.

References

Bilitza, D. (2001). "International reference ionosphere 2000". In: *Radio Science* 36, p. 261.
Dungey, J.W. (1961). "Interplanetary magnetic field and the auroral zones". In: *Phys. Rev. Lett.* 93, p. 47.
Fuller-Rowell, T. J. and D.S. Evans (1987). "Height-integrated Pedersen and Hall conductivity patterns inferred from TIROS–NOAA satellite data". In: *J. Geophys. Res.* 92, p. 7606.
Heelis, R.A., J.K. Lowell, and R.W. Spiro (1982). "A model of the high-latitude ionospheric convection pattern". In: *J. Geophys. Res.* 87, p. 6339.
Millward, G.H. et al. (2001). "An investigation into the influence of tidal forcing on F region equatorial vertical ion drifts using a global ionosphere-thermosphere model with coupled electrodynamics". In: *J. Geophys. Res.* 106, pp. 24,733.
Rawer, K., D. Bilitza, and S. Ramakrishnan (1978). "Goals and status of the international reference ionosphere". In: *Rev. Geophys.* 16, p. 177.
Richmond, A.D., E.C. Ridley, and R.G. Roble (1992). "A thermosphere/ionosphere general circulation model with coupled electrodynamics". In: *Geophys. Res. Lett.* 19, p. 369.
Ridley, A. J., Y. Deng, and G. Tòth (2006). "The global ionosphere-thermosphere model". In: *J. Atmos. Sol-Terr. Phys.* 68, p. 839.
Schunk, R. W. et al. (2004). "Global Assimilation of Ionospheric Measurements (GAIM)". In: *Radio Sci.* 39, doi:10.1029/2002RS002794.
Shim, J.S. et al. (2014). "Systematic evaluation of ionosphere/thermosphere (IT) models: CEDAR electrodynamics thermosphere ionosphere (EIT) challenge (2009-2010)". In: *Modeling the Ionosphere-Thermosphere* 201, p. 145.
Weimer, D. R (2005). "Improved ionospheric electrodynamic models and application to calculating Joule heating rates". In: *J. Geophys. Res.* 110, p. 05306. DOI: 10.1029/2004JA010884.